Synthesis, Structural and Optical Properties of Li-Doped Molybdenum and Vanadium Oxide Nanocrystalline Films

F.A.Ibrahim

Physics Department, Faculty of Science, Suez Canal University, El-Arish branch, El-Arish, Egypt.
E-mail: fahmed_ibrahim@yahoo.com

X-ray diffraction (XRD) and optical properties of (x)Li_2O-(80-x)V_2O_5-(20)MoO_3 (where $0 \leq x \leq 13$ mol.%) films were studied. A sol–gel method (colloidal route) based on $V_2O_5 \cdot nH_2O$ hydro-gel was developed to synthesize these films. X-ray diffraction (XRD), was used to identify the structure of the obtained nanocrystals. Homogenous nanocrystals of 7.6 nm in size was obtained. Optical measurements were carried out using a double-beam spectrophotometer. The optical constants such as refractive index n, the extinction coefficient k, absorption coefficient α, and optical band gap have been evaluated. The optical spectra of some samples exhibited two distinct regions: one at high energy, which suggests a direct forbidden transition with optical gap increases with increase in Li-content. and other at low-energy band, suggests a direct allowed transition with optical gap ranging from 0.40 to 0.50 eV. Additional calculations applying the real part of the optical dielectric function led to the evaluation the ratio of the charge carrier concentration and their effective mass. The sol–gel method is fit for the preparation of (x) Li_2O-(80-x)V_2O_5-(20)MoO_3 material which may offer some favorable properties for commercial application.

1. Introduction

Thin films of V_2O_5 can be prepared by a variety of techniques including: sputtering, vacuum evaporation, pulsed laser ablation, plasma-enhanced chemical vapor deposition, and sol-gel deposition [1-5]. Recent work on lithium insertion reactions from organic electrolyte solutions into oxide materials has focused primarily on the utility of such reactions for secondary battery applications. Most of the studies concentrated on aspects such as the intercalation mechanism, charge density and cycling properties of metal oxide electrodes. Numerous insertion intercalation materials have been proposed as positive electrode material but rather revealed as candidate for negative electrode materials in rechargeable lithium ion batteries. The lithium vanadate Li V O is an example of an insertion compound to be used as positive electrode, in which the lithium ions function as pillars between the vanadium oxide units. They stabilize the oxide structure during the insertion reinsertion process and optimize the space between the vanadium oxide units [6].

Lithium-ion batteries have been considered as an attractive phones, notebook computers, camcorders, electric vehicles, etc. The cathode is particularly critical in determining the discharge capacity of lithium-ion batteries, as it is a crucial component, and has the greatest potential for improvement. Many cathode materials have been explored to satisfy the commercial application. Among the cathode materials, Li_2CO_3, spinel $LiMn_2O_4$ and their substituting derivative compounds are currently used in lithium-ion batteries, but alternative cathode materials have been pursued to replace the oxidative unstable lithium transition metal oxide [7]. In addition, Li_2O doped molybdenum and vanadium oxide nanotubes were prepared by a modified sol–gel process and used as the cathodic material for Li ions battery. Sol-gel method is the preferred thin film technique for many applications. It lends itself to the production of thin layers of metals, oxides, etc. Based on the hydrolysis and condensation of molecular precursors, the sol–gel process offers a route for the low temperature synthesis of oxide materials. Mainly there are two chemical processes that are currently used to prepare sol–gel and depends on the nature of the molecular precursor. These are the inorganic route with metal salts in aqueous solutions or the metal-organic route with metal alkoxides in organic solvents [8].

The main aim of the present work is to investigate two subjects. First the $(x)Li_2O$-$(80-x)V_2O_5$-$(20)MoO_3$ films is proposed. Second is to investigate the compositional dependence on it's optical properties of films under investigation.

2. Experimental Techniques

Fore different compositions of (x) Li_2O-$(80-x)V_2O_5$-$(20)MoO_3$, (where $0 \leq x \leq 13$ mol%), have been proposed for the present investigation. These compositions were synthesized from highly pure vanadium pentoxide (V_2O_5), molybdenum oxide (MoO_3) lithium carbonate (Li_2CO_3). Films of the investigated compounds were prepared by the sol–gel technique. The powders of vanadium pentoxide (V_2O_5) (99.99%), molybdenum oxide (MoO_3) (99.99%) and lithium carbonate (Li_2CO_3) (99.99%) in suitable proportions (mol%) were used as starting materials to prepare precursor. $V_2O_5.nH_2O$ hydro-gel was firstly prepared by sol–gel technique (colloidal route). The sol–gel synthesis ensures homogeneity of the precursors and improved reactivity. The films were prepared by dissolving V_2O_5 and MoO_3 powder in hydrogen peroxide, H_2O_2, solution and dissolving Li_2Co_3 powder in distilled water H_2O, and the stirring continued until became pure solution. The resulting solution was added with different amounts to the above resulting mixture and strongly stirred at 60C temperature. Red brown viscous gels, or colloidal solutions are formed within few days by heating the solution at 60C. Dip coating method was used to form the film on clean 1.5 mm thick high quality Pyrex glass substrates. The film was made in a coplanar geometry and dried spontaneously in ambient conditions to orient the layered plane. X-ray diffraction (XRD) patterns on the other hand were obtained in order to identify the structure and the particle size of the prepared under-test films using XRD Philips P.W.1390 diffractometer with a Cu Kα target and Ni filter. The diffraction data were

recorded for 2θ between 5° and 45°. Optical properties of the films were determined in the semiconductor and metallic states by measuring spectral reflectance at near normal incidence in the wavelength range (190-2500 nm) using a JASCO (V-570) spectrophotometer. Measurements were made with reference to a substrate. The film thickness were measured by an optical based technique using double beam spectrophotometer.

3. Results and Discussion

3.1. X-ray diffraction

The XRD patterns of the present samples are shown in Fig. (1). All X-ray spectra exhibited a deviation in relative peak intensity compared to the standard pattern of orthorhombic V_2O_5 (a = 1.1512 nm, b = 0.3564 nm, c = 0.4368 nm; SG = Pmmn, JCPDS 42–1467).

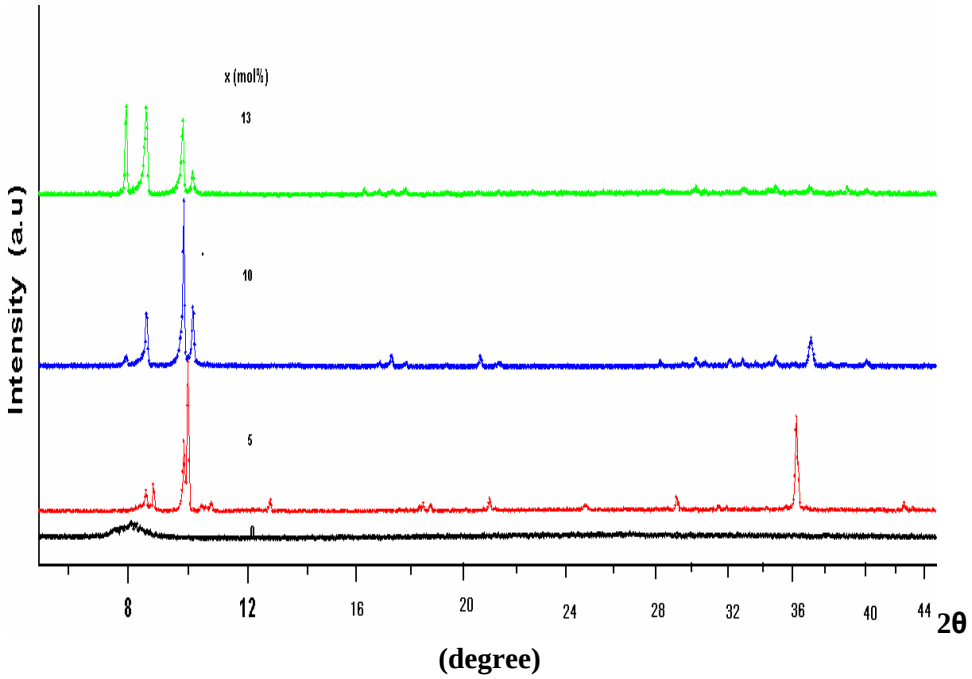

Fig. (1): XRD of (x)Li_2O-(80-x)V_2O_5-(20)MoO_3 films grown on Pyrex glass substrate and measurements at room temperature

The present results indicate that all peaks of (x)Li_2O-(80-x)V_2O_5-(20)MoO_3, films become sharp, suggesting the grains coarsening. The average crystal sizes, D, of the precipitated nanocrystals were calculated according to Sherrer's formula [15]:

$$D = k\lambda / \beta \cos \theta \quad (1)$$

D was found to be on the average 7.6 nm. Where k ~ 1, λ(nm) represents the wavelength of Cu Kα radiation; θ is the Bragg angle of the X-ray diffraction peak and β represents the corrected full width at half maximum of the diffraction peak in radians. The correction was done automatically according to fixed parameters due to experimental broadening. These results indicate that a highly bounded material to the glass substrate with nanocrystalline films, these films can be prepared without any difficulties by the sol–gel technique.

3.2. Film thickness

Film thickness measurements were done after preparation using spectrophotometric method [16]. The spectrophotometric method employed a double-beam recording method. Here the light is incident at an angle θ from a medium of index n_o onto a film of index n_1 and thickness d, deposited onto a substrate of index n_2, with n_1 lying between n_o and n_2. The reflected light shows an interference maximum for a wavelength, λ, when the path difference of $2n_1 d \cos\theta$ between the successive beams reflected at each surface is equal to m_l, where m is an integer. If n_1 is greater than n_o and n_2, then the reflected intensity will show a minimum (dark band results) when $2n_1 d\cos\theta = (m-1/2)\lambda$ and show a maximum if $2n_1 d\cos\theta = (m)\lambda$.

Table (1): Film thicknesses for the system $(x)Li_2O$-$(80-x)V_2O_5$-$(20)MoO_3$

Li %	Thickness (nm)
0	248.8
5	923.4
10	1048.8
13	1348.8

The spectrophotometer is used to measure the transmitted and/or reflected intensity of the normal to the surface beam as a function of wavelength, and also accordingly record the positions of maxima and minima. If m is the order maximum occurring at λ_1 and (m+1) the order at λ_2, we have for normal incidence

$$2n_1 d = m\lambda_1 \quad (2)$$

$$2n_1 d = (m+1)\lambda_2 \quad (3)$$

From Eqs. (2) and (3) we have

$$m = (\lambda_2) / (\lambda_1 - \lambda_2) \quad (4)$$

So the film thickness can be calculated as following:

$$d = (\lambda_1 \lambda_2) / 2n_1 (\lambda_1 - \lambda_2) \quad (5)$$

Thus, with this method we can determine d if n_1 is known [16].

Optical techniques are usually the preferred method for measuring thin films thickness because they are accurate and non- destructive. Applying the above given method films thicknesses are evaluated accordingly and given in Table 1.

3.3. Optical Properties

Usually the optical absorption coefficient, α, is presented by the relation [12]:

$$\alpha(h\upsilon) = A(h\upsilon - E_{Opt})^n \tag{6}$$

and to describe the absorption edge. While within the intermediate absorption region it is described by:

$$\alpha(h\nu) = \alpha_o \exp\left(h\nu / E_o\right) \tag{7}$$

where A is a constant, E_{opt} is the extrapolated optical gap, h is the Plank constant, ν is the frequency of the incident radiation and E_o present the width of localized states at the band edge associated with the amorphous state and is often called the Urbach energy [12].

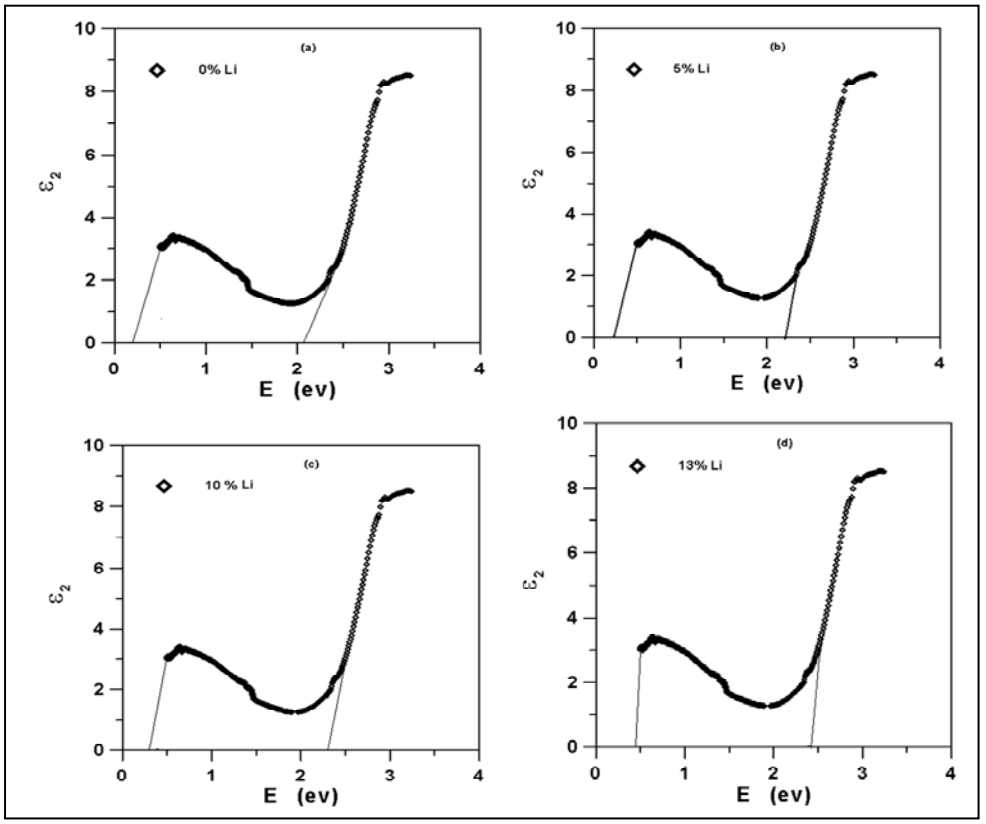

Fig. (2 a,b,c&d) The imaginary part of the dielectric constant ε_2 as a function of photon energy *(hv)* for (a) 0% Li, (b)5% Li, (c) 10% Li and (d)13% Li content.

The exponent *n* may have any of the values 3, 2, 3/2 or 1/2 depending on the nature of the conduction mechanism, either it is indirect or direct, forbidden or allowed, respectively [12].

It is usually more reliable to study the absorption band profile [12] before applying Eqs. (6) and (7). The absorption band is best given by a plot of ε_2 of the complex dielectric permittivity, $\varepsilon^* = \varepsilon_1 - i\varepsilon_2$, as a function of the incident energy, hν. As shown in Fig.(2), there are two independent absorption bands. The first one has a band edge at 2.11-2.43 eV and band tail around of 0.50 eV, while the second band have an edge at 0.25-0.46 eV, i.e. xLi_2O -$(20-x)V_2O_5$-$80MoO_3$ nanocrystalline thin films have more than one type of conduction. The best extrapolated linear fitting to the data at the band edge and intersecting with the, E, x-axis as shown in Fig. (2 a,b,c&d) will give the value E_{opt}. It is noted that the first high energy band gives E_{opt1}~(2.11 - 2.43) eV and is characterized by an indirect allowed transition with n=2. While the second region for hν <0.5 eV is best presented by an absorption band with a gap of E_{opt2}~0.25-0.46 eV, see Fig. (2). This low energy absorption is associated with the transitions involving deep impurity states within the energy gap or to a second gap of lower energy and is described by a direct allowed transition, n =1/2.

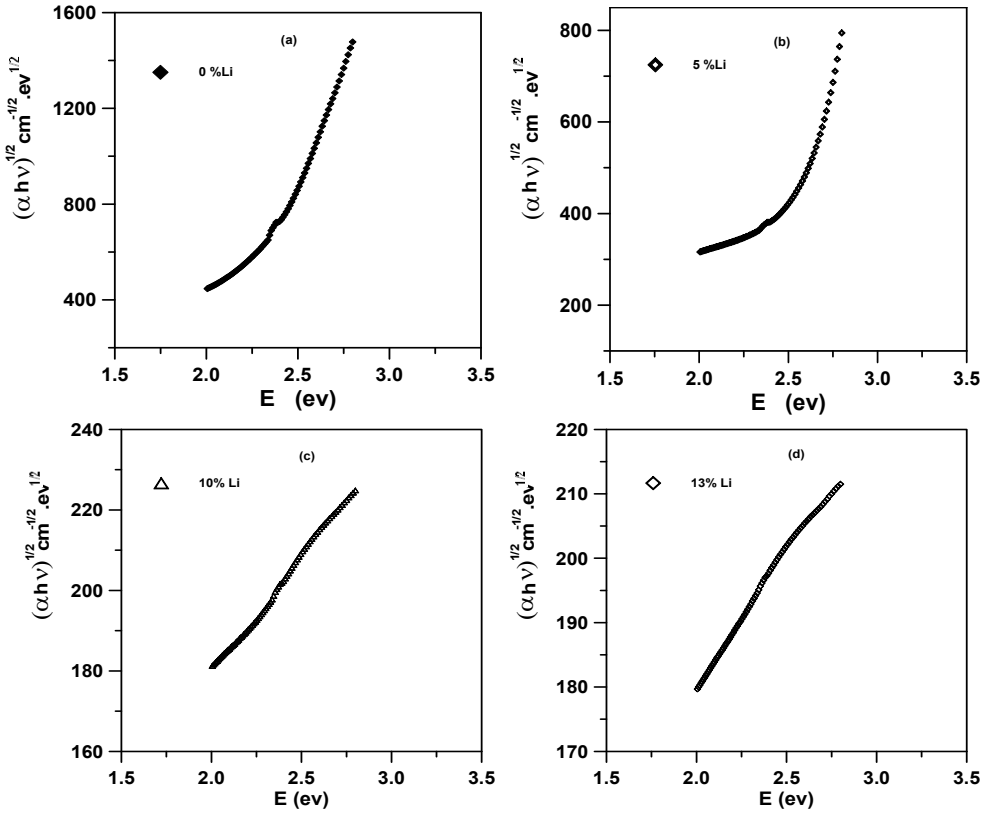

Fig.(3 a,b,c&d): Dependence of $(\alpha h\nu)^{1/2}$ on the photon energy $(h\nu)$ for xLi_2O - $(20-x)V_2O_5$-$80MoO_3$ films with different Li content.

The bands gap obtained here for 0%Li are in a good agreement with the results of similar composition prepared by the electron beam evaporation technique [13]. Finally, it should be noted that any variation in the band gap might be related to the degree of ordering in $(x)Li_2O$-$(80-x)V_2O_5$-$20MoO_3$ (where $0 \leq x \leq 13$ mol.%) films arrangement. It is clear from the electrical conductivity results [3] and the optical gap, that we have, $E_{opt2}=2W$, indicating an n-type intrinsic semiconductor.

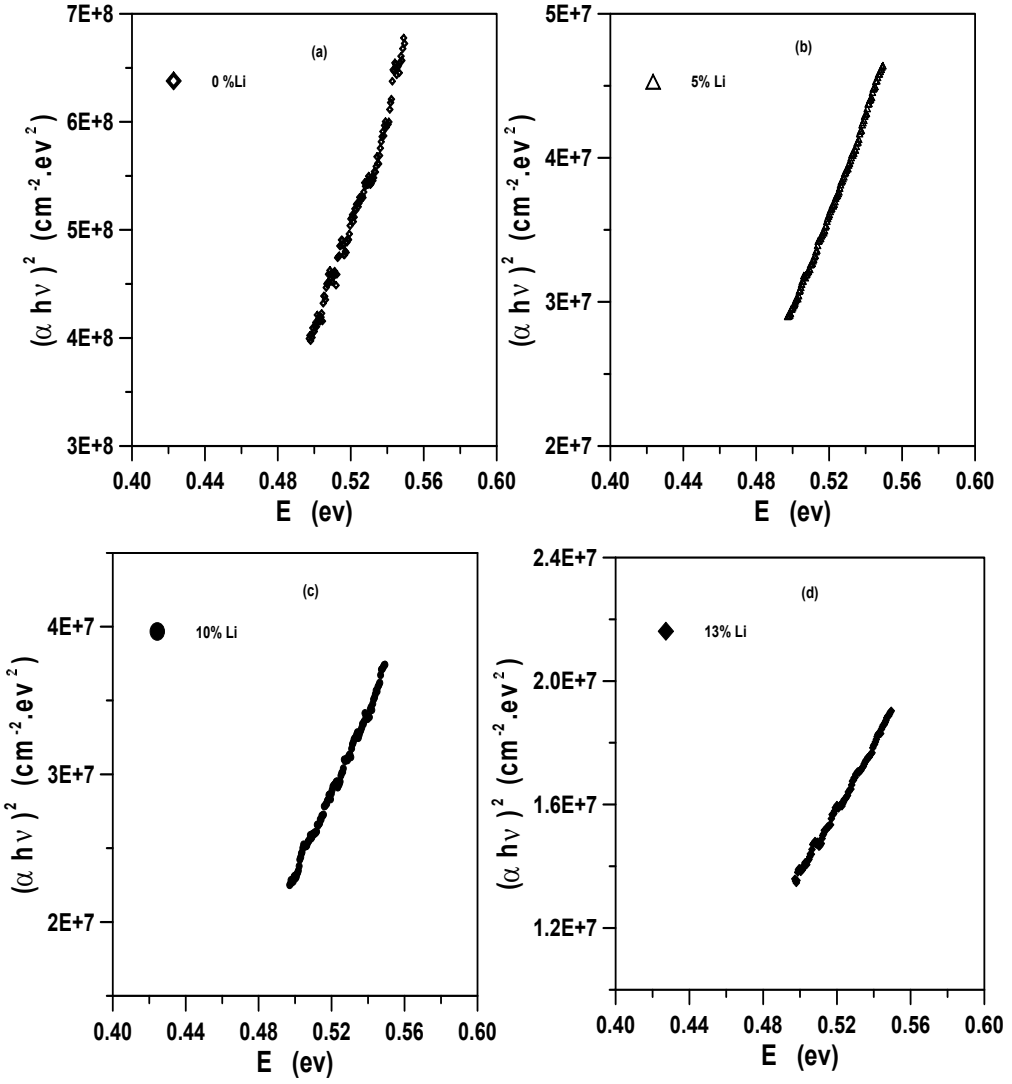

Fig.(4 a,b,c&d): Dependence of $(\alpha hv)^2$ on the photon energy (hv) for xLi_2O -$(20-x)V_2O_5$-$80MoO_3$ films with Li content.

Table (2): Optical constant (E_{Opt} , ε_∞ & N/m^*) of xLi_2O -(20-x)V_2O_5-80MoO_3 (where $0 \leq x \leq 13$ mol.%) films as a function of compositions and thickness.

Li%	(d) (nm)	E_{Opt1} (eV)	E_{Opt2} (eV)	ε_∞	N/m^* ($m^{-3}.kg^{-1}$)
0	248.8	2.11	0.25	2.11	$2.53x10^{24}$
5	923.4	2.25	0.28	5.51	$4.24x10^{23}$
10	1048.8	2.34	0.32	3,62	$4.87x10^{23}$
13	1338.8	2.43	0.46	3.01	$5.28x10^{23}$

From Table (2), it is clear that the optical gap E_{Opt} increases with increase Li content.

Furthermore the optical spectra may be applied to evaluate, ε_∞ , and N/m^* by applying the real part dielectric constant, ε_1, of the complex dielectric constant [16] as:

$$\varepsilon_1 = \varepsilon_{\infty 1} - \frac{e^2 N}{\pi \varepsilon_o m^* c^2} \lambda^2 \qquad (8)$$

where ε_1 is the real part of dielectric constant, ε_∞ is the lattice dielectric constant, λ is the wavelength, e is the charge of the electron, N is the free charge-carrier concentration, ε_o is the permittivity of the free space, m* the effective mass of the electron and c is the velocity of light It is observed that the dependence of ε_1 on λ^2 is linear at longer wavelengths, is shown in Fig. (5).

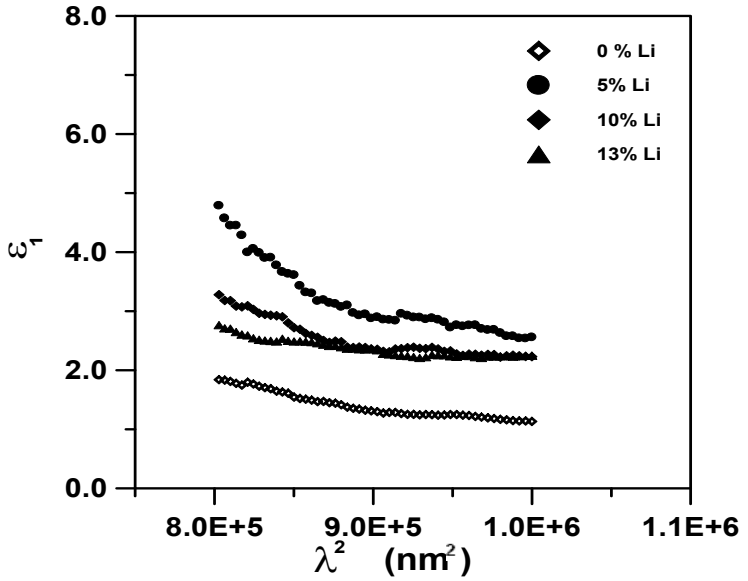

Fig. (5): Plots of ε_1 against λ^2 for films of xLi_2O -(20-x)V_2O_5-80MoO_3 (where $0 \leq x \leq 13$ mol.%) system

Extrapolating the linear part of this dependence to zero wavelength gives the value of ε_∞ and from the slopes of these lines we can calculate the values of N/m^* for the investigated films. Values of ε_∞ and N/m^* are given in Table (2).

4. Conclusions

A water-soluble lithium compound added to the aqueous sol (derived from V_2O_5 and MoO_3 powder) was used dip coating method to form the films on glass. XRD diffraction measurements show that, xLi_2O -(20-x)V_2O_5-80MoO3 thin films are nanocrystals. Optical measurements revealed that there are two different optical gaps present. E_{op1} suggests a direct forbidden transition with optical gap in the range 2.11–2.43eV.On the other hand E_{op2} suggests an inter-band direct allowed transition with an optical gap in the range 0.25–0.46 eV. The optical gap was found increase with increase in Li-content. The carrier's concentrations over the effective mass were calculated.

Acknowledgement

The author thank Prof. M. M. El-Desoky Department of Physics Faculty of Science Suez University - Suez, Egypt, for Scientific and significant Support.

References

1. A.A. Bahgat, F.A. Ibrahim, M.M. El-Desoky, *Thin Solid Films*, **489**, 68 (2005).
2. A.A. Bahgat, F.A. Ibrahim, M.M. El-Desoky, *AIP Conf. Proc*., **1370**, 61 (2011).
3. M.M. El-Desoky, F.A. Ibrahim, *J. Sol-Gel Sci Technol*., (2011).
4. M.S. Al-Assiri , M.M.El-Desoky, A.Alyamani, A.Al-Hajry, A.Al-Mogeeth, A.A.Bahgat, *Optics & Laser Technology*, **42**, 994 (2010).
5. M. S. Al-Assiri, M. M. El-Desoky, A. Alyamani, A. Al-Hajry, A. Al-Mogeeth, A. A. Bahgat, *Philosophical Magazine*, **3421** (2010).
6. V. Serge, Pouchko a,), Alexey K. Ivanov-Schitz a, Frans G.B. Ooms b, Joop Schoonman b . *Solid State Ionics*, **144**, 151 (2001).
7. Yuzhan Li, Zhen Zhou, Manman Ren, Xueping Gao, Electrochimica Acta **51**, 6498 (2006).
8. T.J. Hanlon*, J.A. Coath, M.A. Richardson., *Thin Solid Films*, **436**, 269 (2003).
9. J.I. Pankove, "*Optical Processes in Semiconductors*", (Englewood Cliffs, New Jersey, 1971).
10. J. Tauc, "*Amorphous and Liquid Semiconductors*", (Plenum Press, New York, 1974).
11. M. L. Theye, *J. Non-Crystalline Solids*, **164**, 1262 (1993).

12. N.F. Mott and E.A. Davis, "*Electronic Process in Noncrystalline Materials*", (Clarendon Press, Oxford, 1971).
13. K. V. Madhuri, B. S. Naidu, O.M. Hussain, M. Eddrief, and C. Julien, *J, Materials Science and Engineering* B **86**, 165 (2001).
14. P. T. Deshmukh, D. K. Burghate, V. S. Deogaonkar, S. P. Yawale and S. V. Pakade, *J. Bull. Mater. Sci*., **26**, 639 (2003).
15. D. Lou, N. Audebrand, *Adv. X-ray Anal*., **41**, 556 (1997).
16. Pankove I. Optical processes in semiconductors. New Jersey: Prentice-Hall Inc.; (1971).